Effects of thermal history and microstructure on grain boundary segregation in the heat-affected zone of an Alloy182-A533B dissimilar weld joint

Graduate School of Engineering, Tohoku University	Ziqing ZHAI	Member
Central Research Institute of Electric Power Industry	Yuichi MIYAHARA	Non- member
Graduate School of Engineering, Tohoku University	Hiroshi ABE	Member
Graduate School of Engineering, Tohoku University	Yutaka WATANABE	Member

Grain boundary (GB) segregation of phosphorus and alloying elements in the heat-affected zone (HAZ) of an Alloy182-A533B dissimilar weld joint used in nuclear reactor pressure vessels was studied quantitatively by three-dimensional atom probe tomography. Non-equilibrium segregation occurred during welding and post-weld heat treatment, leading to remarkable enrichment of P, C, Mn and Mo at GBs, of which the levels were all microstructure- dependent. After step cooling, P and Mn showed further increase at GBs through equilibrium segregation, while decrease in the GB content was observed for C and Mo. The results indicated increasing susceptibility of temper embrittlement of HAZ in progress with service time.

Keywords: grain boundary segregation; low alloy steel; atom probe tomography; thermal history; heat-affected zone microstructure.

1. Introduction

The toughness of low alloy steels (LAS) can be degraded by ageing, which increases the ductile-brittle transition temperature by an amount dependent on material, prior heat treatment, ageing temperature and time. This embrittlement is associated with segregated elements at grain boundaries (GB), essentially phosphorus (P) [1, 2]. Due to the specific thermal cycles induced by multi-pass welding, complex phase transformations take place in the heat-affected zone (HAZ) of LAS, especially in the close vicinity of the fusion boundary (FB), resulting in coarse-grained (CG), fine-grained (FG), intercritically reheated coarse-grained (ICCG) and subcritically reheated coarse-grained (SCCG) HAZ [3]. Variations of solute segregation at GBs are also expected in these microstructures. Although the fundamentals of the interactive co-segregation of P and alloying elements in thermally aged ferritic steels have been extensively studied, little is known about the actual segregation behaviors in a weldment with complex thermal histories. In order to evaluate and mitigate the risks of temper embrittlement induced by thermal ageing, a better understanding on the segregation in weldments is necessary. In this study, a systematic quantitative characterization on the GB segregation of P and alloying elements in the HAZ of a LAS was carried out using three-dimensional atom probe tomography (3D APT), with focuses on the effects of thermal history and HAZ microstructure. Characteristics of interactive co-segregation between P and some alloying elements were also examined.

Corresponding author: Ziqing Zhai
Address: 6-6-01-2 Aoba, Aramaki, Aoba-Ku, Sendai 980-8579, Miyagi
Email: ziqing.zhai@rbm.qse.tohoku.ac.jp

2. Experimental

2.1 Material and Specimen Preparation

The HAZ investigated in this study was fabricated by filling Ni-based alloy 182 into a machined groove in an A533B plate using shielded arc welding. The chemical composition of the LAS is given in Table 1. A typical post-weld heat treatment (PWHT) was applied to reduce residual stresses present after the welding and fast cooling process. This consisted of 25 h at 615 ºC and cooling to 315 ºC with a cooling rate of ~180 ºC/h in still air, followed by cooling to room temperature after being pulled out from the furnace. An additional step cooling treatment was conducted on part of the weld joint to promote P segregation [4]. The sequence for this process was 593 ºC/1 h → 538 ºC/15 h →524 ºC/24 h →

Table 1 The chemical compositions of the A533B base material

Element	C	Si	P	S	Mn	Mo	Ni	Cr	Cu	Ti	V	Fe
Concentration (wt.%)	0.20	0.24	0.009	0.004	1.41	0.54	0.65	0.13	0.12	0.001	0.001	Bal.
Concentration (at.%)	0.91	0.24	0.016	0.007	2.75	0.31	0.61	0.14	0.10	0.001	0.001	Bal.

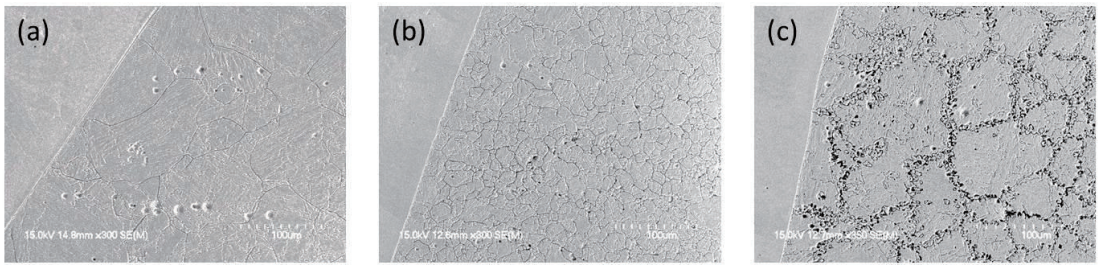

Fig.1 HAZ microstructures in the immediate vicinity of the FB: (a) CGHAZ, (b) FGHAZ, and (c) ICCGHAZ

496 ºC/48 h → 468 ºC/125 h.

Most of the APT samples from the CGHAZ, FGHAZ and ICCGHAZ were prepared separately by a modified two-stage electropolishing method. The morphology of these three microstructures is presented in Fig.1. The sample preparation procedure is detailed elsewhere [5]. It should be noted that by using the two-stage electropolishing method, GBs can only be found through random encounters and their exact natures are unknown. Since P is one of the targeted segregants in this study and it is reported that P tends to favor PAGBs and high angle packet boundaries for segregation [6, 7], it seems reasonable to assume that the boundaries found with enriched P by APT tests belong to these two categories (hereafter referred to as grain/packet boundaries (G/PB)).

2.2 The APT Tests and Analysis

APT tests were performed using a Cameca local-electrode atom probe (LEAP) 3000HR operating in high voltage mode, with a pulse repetition rate of 200 kHz, a 15% pulse fraction, and a sample temperature of 50 K. The number of G/PBs observed in the base material (BM), CGHAZ, FGHAZ and ICCGHAZ of non step-cooled (NSC) and step-cooled (SC) samples are 2, 4, 3, 5 and 2, 2, 1, 2 respectively. 3D reconstruction and data analysis of these samples were performed with Imago Visualization and Analysis Software (IVAS), version 3.6.

In order to quantify solute segregation at G/PBs, a minimum of 7 cylinders with identical diameters of 3 nm were sampled randomly over the interface and normal to the local interfacial plane. One-dimensional (1D) compositional profiles were plotted along the axial direction of these cylinders at a bin size of 70 atoms. These profiles were further transformed to ladder diagrams [8], which display the variation between the accumulated solute atoms along the 1D volume as related to the total accumulation of all atoms. Segregation of the solutes of interest was then quantified in terms of Gibbsian interfacial excess (GIE) [9]. This method is based on the assumption that the compositions of the two adjacent regions are constant up to the dividing surface and that the interface has negligible volume, which is adequate for the estimation of equilibrium segregation (ES). However, welding/PWHT and the subsequent cooling occurred in materials can lead to non-equilibrium segregation (NES), a mechanism that relies on the formation and diffusion of vacancy-solute complexes [10] and strongly depends on grain size, start temperature, cooling rate and time [11]. This process does not only influence the composition at GBs but also their vicinities, resulting in a wider spread of segregation compared to ES. Therefore, the width of the solute segregated zone W_{seg}, represented by the highest solute concentration region in ladder diagrams was also measured in order to investigate the segregation mechanism of the solutes of interest.

3. Results and Discussions

3.1 Effects of Welding/PWHT and Subsequent Cooling on Solutes Segregation at G/PBs

Segregation of various solutes at G/PBs was found in the BM and all HAZ microstructures both before and after

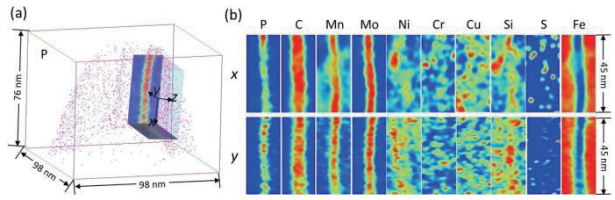

Fig.2 Distribution of solutes in the vicinity of a G/PB in NSC-ICCGHAZ

step cooling. Fig.2 displays the cumulative two-dimensional (2D) concentration maps of various solutes across a G/PB found in NSC ICCGHAZ. While Ni and Si only show ambiguous or marginal segregation, P, C, Mn and Mo are clearly enriched at the interface. No evidence of Cr, Cu or S segregation is observed. Similar phenomena were also found in SC materials.

Fig.3 summarizes the observed relationship between the W_{seg} and φ, the angle between the local G/PB plane and the axial direction of the sample, in all investigated microstructures for P, C, Mn and Mo. The results show that for all the solutes examined, the W_{seg} gradually decreases with φ and becomes smallest when $\varphi = 90°$. This is in agreement with the work of Maruyama and is attributed to the local magnification effect [12]. Despite of this artificial effect, an approximately constant difference in the W_{seg} of P and Mo as a function of φ is visible between NSC and SC materials. On the contrary, the W_{seg} of C and Mn show little change before and after step cooling. It should also be noted that the value of W_{seg} differs with solute species, where the W_{seg} of P is evidently narrower than the W_{seg} of C, Mn and Mo

The average GIE of P, C, Mn and Mo at G/PBs with respect to microstructures are presented in Fig.4. For NSC materials, the segregation level of P, C, Mn and Mo are more elevated at the G/PBs in CGHAZ and ICCGHAZ than in FGHAZ. These features are consistent with NES, which is believed to be microstructure-dependent [11, 13]. The NES in the observed materials probably occurred during the phase transformation induced by welding and subsequent cooling, as well as PWHT followed by fast cooling from 615ºC to 315ºC. Since the G/PBs in BM exhibit similar segregation level with those in FGHAZ for almost all the solutes examined, welding seem to have more profound impacts on the segregation level of solutes at G/PBs than PWHT. Larger grains, higher start temperature and faster cooling rate tend to result in higher segregation level at G/PBs. One explanation is that the smaller grain size in BM and FGHAZ increases the total volume of G/PBs, thus provides more defect sinks for segregation. It is also possible that desegregation takes place at the smaller grain sizes, leading to lower segregation level at G/PBs in these regions. Additionally, in contrast to the large amount of PAGBs existing in CGHAZ and ICCGHAZ, most PAGBs in FGHAZ transform into ferrite GBs by heating up the material during the second weld pass to

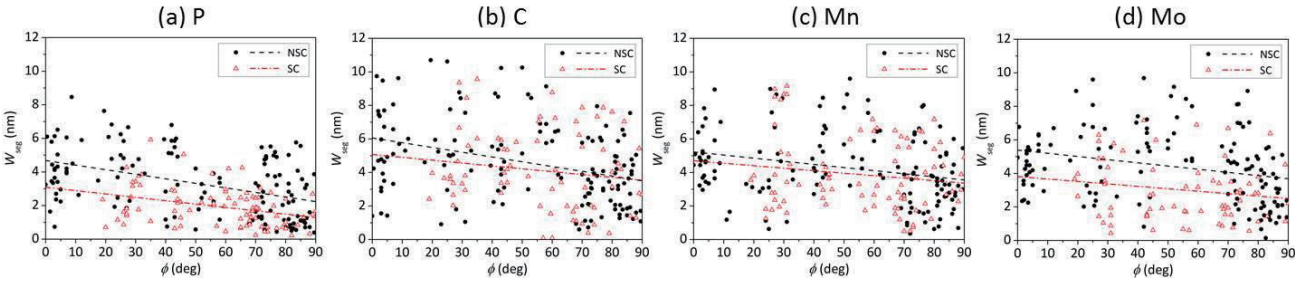

Fig.3 Distribution of the W_{seg} of P, C, Mn and Mo at G/PBs before and after step cooling with respect to φ.

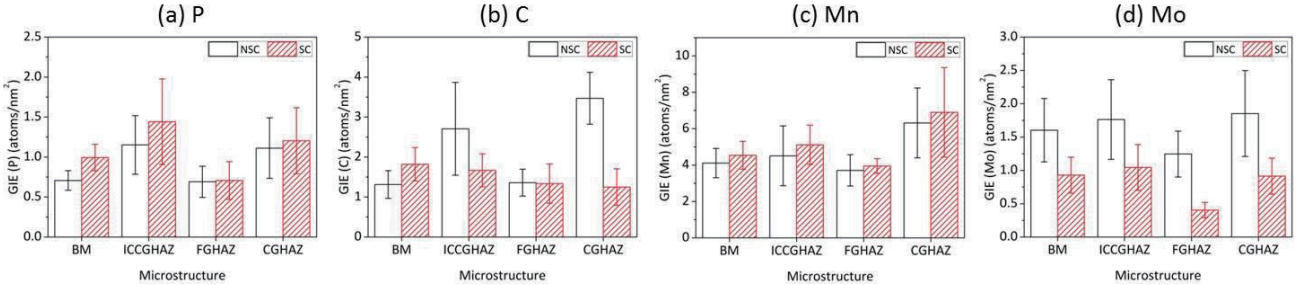

Fig.4 The estimated GIE of P, C, Mn and Mo at G/PGs with respect to different types of microstructure.

over ~900ºC and cooling at a slower rate from a lower start temperature [3, 11]. As higher segregation level of Nb at PAGBs than at ferrite-ferrite GBs has been reported [14], it seems that segregation level of solutes may vary with the type of GB. More detailed study is needed to attain a better understanding on the role of the type of GBs in solutes segregation in LAS.

3.2 Effects of Step Cooling on Solutes Segregation at G/PBs

Step cooling showed opposite effects on P, Mn compared to C, Mo. While slight increase in the segregation level is observed for P and Mn, significant decrease occurs in the segregation level of C and Mo in almost all the microstructures. Correlation between Fig.3a and Fig.4a reveals that, some P atoms close to the interface after NES reach the G/PB plane during ES induced by step cooling, leading to a narrower W_{seg} of P. Meanwhile, some long range diffusion also takes place, resulting in higher segregation level of P after step cooling. On the other hand, Fig.3c suggests that the influence of ES on Mn is not very high although increased segregation level of Mn was found after step cooling. A possible explanation is that the enrichment of P at G/PBs during ES promoted Mn segregation through interaction. In contrast, the content of C and Mo at G/PBs decreased during step cooling. It may indicate that the maximum ES level of C and Mo are lower than the segregation level resulted by the prior heat treatments, thus causing these two types of solute to desegregate and reducing their final amount at G/PBs. The noticeable difference in the W_{seg} of Mo before and after step cooling is indicative of a faster desegregation rate compared to that of C, which shows little change in the W_{seg} during NES and ES. This may be attributed to the different diffusion mechanism of interstitial (C) and substitutional (Mo) atoms [15].

In addition, C and Mo have been identified as the two principal segregants at dislocations encountered in the APT tests. The dislocations probably form on slip planes within individual grains, and generally appear in long, thin and slightly curved strip shape, as presented in Fig.5(a). Although the exact density of dislocations is unknown, such features are quite commonly encountered in almost all microstructures including the BM and HAZ in both the NSC and SC materials. As shown in Fig.5(b) and (c), the concentrations of C and Mo at dislocations vary from site to site, which may depend on the type of dislocations [16]. To investigate the effects of step cooling on the composition of dislocations, a 0.3 atoms/nm^3 C + Mo iso-density surface was selected to delineate the dislocations, and the concentration of C and Mo enclosed by the iso-density surfaces were measured. In total, 43 and 49 dislocations were investigated for NSC and SC materials, respectively. The average concentration before and after step cooling are 0.94 ± 0.38 at.% and 0.66 ± 0.22 at.% for C, and 0.55 ± 0.39 at.% and 1.12 ± 0.36 at.% for Mo. While slight decrease is observed in the average C concentration at dislocations after step cooling, the average Mo concentration at dislocations is more than doubled. The concentration ratio of C : Mo changes from ~ 1 : 0.6 before step cooling to ~ 1 : 1.7 after step cooling, which is indicative of the onsetting of Mo_2C precipitation.

On the other hand, comparison between the average bulk composition before and after step cooling reveals that, the average bulk C content in the vicinity of G/PBs (< ±100 nm from the G/PB plane) increases from 0.031 ± 0.001 at.% to 0.044 ± 0.002 at.%, while the average bulk Mo content decreases from 0.125 ± 0.003 at.% to 0.077 ± 0.002 at.%. This is consistent with the compositional fluctuation of C and Mo observed at dislocations before and after step cooling. It seems that during step cooling,

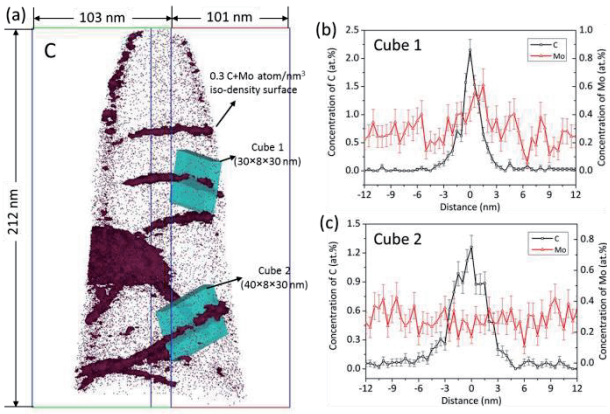

Fig.5 (a) C enrichment at dislocations in a NSC-BF sample, (b) and (c) the 1D compositional profiles across the dislocation sites enclosed by the cubes shown in (a)

competition takes place between ES and precipitation of Mo, and that dislocations act as stronger sinks for Mo than G/PBs. Mo has been reported to reduce temper embrittlement by either tying P atoms up in the grain interior or by counteracting the embrittlling effect of segregated P atoms at GBs [17]. It is likely that in this case, the solubility of Mo in iron is reduced during step cooling due to its affinity for C, thus hampering its scavenging action on P segregation at G/PBs. However, the precipitation/coarsening of Mo rich carbides is strongly dependent on the nominal Mo content, ageing time and temperature [18]. It is necessary to verify these findings by isothermal ageing the material at service temperatures, which are lower than the temperatures applied in step cooling.

3.3 Implications on Synergistic Co-segregation

In order to investigate the existence of co-segregation between different solutes, all G/PBs were extracted from the original APT dataset using a 0.2 atoms/nm^3 C + P iso-density surface, which was chosen because it forms a relatively smooth shell near the inflection point between the interface and the matrix. Examples of the cumulative 2D concentration map of C, Mn, Mo and P plotted along the direction giving the maximum projection area of the interface are displayed in Fig.6. Obviously, the distributions of all the solutes examined are inhomogeneous at the interface. Radial- distribution analysis [8] was implemented on P atoms in all the extracted G/PBs. It examines the average local neighborhood as a function of distance extending radially outwards from each P atom in the datasets. In this study, the thickness of the concentric shells built around each P atom is set as 0.5 nm, which approximately equals to the average 1-order nearest neighbor distance [8] between P-P atoms (~0.5 – 0.75 nm) at G/PBs. Results presented in Fig.7 indicate that Mn and Mo tend to segregate in close proximities of P while C behaves oppositely. These are consistent with the previously reported repulsive C-P interaction and the attractive interaction between the metallic alloying element M and the embrittling impurity I [18]. As Mo alone appears as a very weak segregant at GBs in Fe [19, 20], it seems that the Mo-P interaction is critical for the segregation of Mo. Although strong C-Mo affinity has also been reported [18], such interaction tends to prefer C-enriched dislocations and precipitates but not G/PBs. It is also worthy to note that the concentration distribution of C and Mo as a function of distance to a P atom at G/PBs drop significantly after step cooling, while that of Mn increases. This agrees well with the observed changes in the segregation level presented in

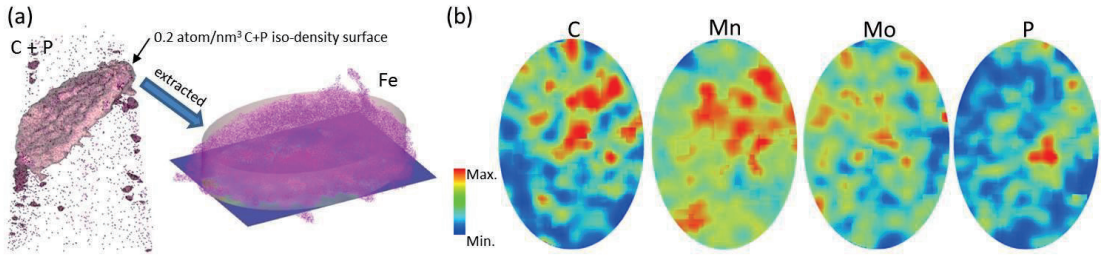

Fig.6 (a) A G/PB in SC-ICCGHAZ extracted by a 0.2 atom/nm^3 C + P iso-density surface, (b) Cumulative 2D concentration maps of P, C and Mo at a G/PB

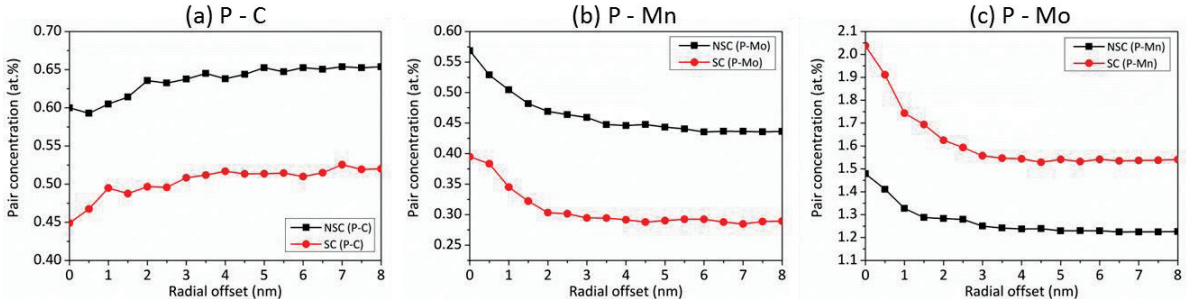

Fig.7 Averaged P-centered C, Mn and Mo radial-distributions from all G/PBs in NSC and SC materials.

Fig.4. As C enhances GB cohesion while P and Mn act oppositely [18, 21], the results suggest increasing risk of temper embrittlement with progress in service time of LAS, especially in the ICCGHAZ and CGHAZ.
On the other hand, similar trends in partial radial-distribution of P-C, P-Mn and P-Mo are observed in both NSC and SC materials, indicating that similar interactions between these solutes occur during the different thermal treatments.

4. Conclusions

In summary, effects of thermal history and microstructure on segregation of P, C, Mn and Mo at G/PBs in the HAZ of a LAS were studied quantitatively using 3D APT. The main conclusions are listed below:
(1) The thermal history of the material, consisting of welding and quenching after welding (causing NES), PWHT at 615ºC for 25 h and cooling to 315ºC (causing ES and/or NES), followed by cooling to room temperature (no significant segregation expected) and step cooling (causing ES), had profound influence on the final segregation level at G/PBs of all the solutes examined.
(2) NES during welding and subsequent cooling appeared to play a vital role in the microstructure-dependent segregation of P, C, Mn and Mo at G/PBs, resulting in higher G/PB enrichment of all the solutes in ICCGHAZ and CGHAZ than in FGHAZ and BM.
(3) The ES induced by step cooling further promoted the segregation level of P and Mn at G/PBs. On the contrary, it led to the desegregation of C and Mo at G/PBs.
(4) Competition between segregation and precipitation of Mo occurred during step cooling. The solubility of Mo in iron appears to be significantly reduced by precipitating at dislocations, contributing to the observed changes in the segregation level of solutes at G/PBs.
(5) Repulsive interaction between P-C, and attractive interaction between P-Mn and P-Mo at G/PBs seem to have taken place during the entire thermal history, which showed good agreement with the interactions observed between these solutes in previous studies.

References

[1] M. Guttmann, "Interfacial Segregation and Temper Embrittlement", in "Encyclopedia of Materials: Science and Technology (Second Edition)", Elsevier, 2001; pp.1 - 8.
[2] C.J. McMahon Jr, "Mechanisms of intergranular fracture in alloy steels", Materials Characterization, Vol.26, 1991, pp.269-287.
[3] J. Katsuyama, T. Tobita, Y. Nishiyama and K. Onizawa, "Mechanical and Microstructural Characterization of Heat-Affected Zone Materials of Reactor Pressure Vessel", Journal of Pressure Vessel Technology, Vol.134, 2012, pp.031402-7.
[4] C. Naudin, J.M. Frund and A. Pineau, "Intergranular fracture stress and phosphorus grain boundary segregation of a Mn-Ni-Mo steel", Scripta Materialia, Vol.40, 1999, pp.1013-1019.
[5] Z. Zhai, Y. Miyahara, H. Abe and Y. Watanabe, "Segregation behavior of phosphorus in the heat-affected zone of an A533B/A182 dissimilar weld joint before and after simulated thermal ageing", Journal of Nuclear Materials, Vol.452, 2014, pp.133-140.
[6] S. Raoul, B. Marini and A. Pineau, "Effect of microstructure on the susceptibility of a 533 steel to temper embrittlement", Journal of Nuclear Materials, Vol.257, 1998, pp.199-205.
[7] A.F. Gourgues, H.M. Flower and T.C. Lindley, "Electron backscattering diffraction study of acicular ferrite, bainite, and martensite steel microstructures", Materials Science and Technology, Vol.16, 2000, pp.26-40.
[8] B. Gault, M.P. Moody, J.M. Cairney and S.P. Ringer, "Atom probe microscopy", Springer, 2012.
[9] M.K. Miller and G.D.W. Smith, "Atom probe analysis of interfacial segregation", Applied Surface Science, Vol.87–88, 1995, pp.243-250.
[10] R.G. Faulkner, "Segregation to boundaries and interfaces in solids", International Materials Reviews, Vol.41, 1996, pp.198-208.
[11] P. Maier and R.G. Faulkner, "Effects of thermal history and microstructure on phosphorus and manganese segregation at grain boundaries in C–Mn welds", Materials Characterization, Vol.51,

2003, pp.49-62.
[12] N. Maruyama, G.D.W. Smith and A. Cerezo, "Interaction of the solute niobium or molybdenum with grain boundaries in α-iron", Materials Science and Engineering: A, Vol.353, 2003, pp.126-132.
[13] P. Lejček, "Grain boundary segregation in metals", Springer, 2010.
[14] P.J. Felfer, C.R. Killmore, J.G. Williams, K.R. Carpenter, S.P. Ringer and J.M. Cairney, "A quantitative atom probe study of the Nb excess at prior austenite grain boundaries in a Nb microalloyed strip-cast steel", Acta Materialia, Vol.60, 2012, pp.5049-5055.
[15] D.A. Porter and K.E. Easterling, "Phase Transformations in Metals and Alloys", Chapan & Hall, 1992.
[16] E.V. Pereloma, I.B. Timokhina, J.J. Jonas and M.K. Miller, "Fine-scale microstructural investigations of warm rolled low-carbon steels with and without Cr, P, and B additions", Acta Materialia, Vol.54, 2006, pp.4539-4551.
[17] P. Dumoulin, M. Guttmann, M. Foucault, M. Palmier, M. Wayman and M. Biscondi, "Role of molybdenum in phosphorus-induced temper embrittlement", Metal Science, Vol.14, 1980, pp.1-15.
[18] M. Guttmann, P. Dumoulin and M. Wayman, "The thermodynamics of interactive co-segregation of phosphorus and alloying elements in iron and temper-brittle steels", Metallurgical and Materials Transactions A, Vol.13, 1982, pp.1693-1711.
[19] R. Guillou, M. Guttmann and P. Dumoulin, "Role of molybdenum in phosphorus-induced temper embrittlement of 12%Cr martensitic stainless steel", Metal Science, Vol.15, 1981, pp.63-72.
[20] P. Dumoulin and M. Guttmann, "The influence of chemical interactions between metallic and metalloid solutes on their segregation in α-Fe I: Co-segregation at free surface studied by Auger electron spectroscopy", Materials Science and Engineering, Vol.42, 1980, pp.249-263.
[21] H.J. Grabke, K. Hennesen, R. Möller and W. Wei, "Effects of manganese on the grain boundary segregation, bulk and grain boundary diffusivity of P in ferrite", Scripta Metallurgica, Vol.21, 1987, pp.1329-1334.